



# *In vivo* imaging of TGF $\beta$ signalling components using positron emission tomography

Lonneke Rotteveel<sup>1</sup>, Alex J. Poot<sup>1</sup>, Harm Jan Bogaard<sup>2</sup>, Peter ten Dijke<sup>3</sup>, Adriaan A. Lammertsma<sup>1</sup> and Albert D. Windhorst<sup>1</sup>

<sup>1</sup> Department of Radiology and Nuclear Medicine, Amsterdam UMC, location VUmc, Amsterdam, The Netherlands

<sup>2</sup> Pulmonary Medicine, Institute for Cardiovascular Research, Amsterdam UMC, location VUmc, Amsterdam, The Netherlands

<sup>3</sup> Department of Cell and Chemical Biology, Oncode Institute, Leiden University Medical Center, Leiden, The Netherlands

The transforming growth factor  $\beta$  (TGF $\beta$ ) family of cytokines achieves homeostasis through a careful balance and crosstalk with complex signalling pathways. Inappropriate activation or inhibition of this pathway and mutations in its components are related to diseases such as cancer, vascular diseases, and developmental disorders. Quantitative imaging of expression levels of key regulators within this pathway using positron emission tomography (PET) can provide insights into the role of this pathway *in vivo*, providing information on underlying pathophysiological processes. PET imaging can also be used to study the drug targeting of this pathway and to detect diseases in which this pathway is disturbed. In this review, we provide an overview of PET tracers available to study the TGF $\beta$  signalling pathway. In addition, we discuss future imaging targets for this pathway and possible leads for new PET tracers.

## Introduction

PET is a quantitative imaging technique to visualise and characterise biological processes *in vivo*, such as receptor expression or specific metabolic pathways [1]. As such, PET can be used to study disease pathophysiology, provide insights into target expression and for drug development (i.e., by measuring drug-induced receptor occupancy) [2]. In addition, PET imaging can not only provide information on the biological processes underlying a disease, but also be used for early detection of that disease and for monitoring response to treatment [3]. Thus, a successful PET tracer can provide information on the distribution of molecular targets and drug interactions *in vivo* and, therefore, can be used in many stages of the healthcare system.

TGF $\beta$  family of cytokines is involved in many cellular (patho)-physiological processes. It contains over 30 structurally related polypeptide growth factors (Table 1) [4]. Members of the TGF $\beta$  family can be found in various tissues of both vertebrates and invertebrates, where they

**Lonneke Rotteveel** received her MSc in drug discovery and safety at the VU University in Amsterdam. She is currently finishing her PhD at the VU University Medical Center (VUmc) under the supervision of A. D. Windhorst and Adriaan A. Lammertsma. Her research interest is on the development of positron emission tomography (PET) tracers that target selectively the activin receptor-like kinase 5 *in vitro* and *in vivo*.



**Alex J. Poot** obtained his PhD in medicinal chemistry from Utrecht University. As postdoctoral researcher at the VUmc, Amsterdam, he developed radiolabelled anticancer drugs for PET imaging. In 2014, he accepted a research fellowship from Memorial Sloan Kettering Cancer Center, New York to develop <sup>13</sup>C-labelled probes for tumour metabolism imaging with magnetic resonance imaging (MRI). In 2015, he was appointed as an assistant professor at the VUmc, where his research focusses on novel radiolabelling methods with carbon-11 and fluorine-18, and the application of radiolabelled drugs for oncology PET imaging.



**Albert D. Windhorst** received his PhD degree in radiopharmaceutical chemistry in 1998 and was appointed as chair of radiopharmaceutical chemistry in 2014 at VUmc. His research interests are in the development of new radiolabelling methods for fluorine-18 and carbon-11, the application of these new techniques to the synthesis of PET tracers for oncology, neurology, and cardiology, and the translation of these new PET tracers to clinical research. He is immediate past president of the Society of Radiopharmaceutical Sciences, editor of *Journal of Labelled Compounds & Radio-pharmaceuticals* and associate editor of *Nuclear Medicine & Biology*.



Corresponding author: Rotteveel, L. (l.rotteveel@amsterdamumc.nl)

TABLE 1

**Individual components of the TGF $\beta$  family signalling pathways, including ligands, type I and type II receptors, and intercellular SMAD effectors and inhibitory SMADs<sup>a</sup>**

Component	TGF $\beta$ pathway	Activin/inhibin/Nodal pathway	BMP pathway
Ligands	TGF $\beta$ 1/2/3	Activin A/B, Inhibin A/B	BMP2/4–10
Type I receptors <sup>b</sup>	ALK5 (T $\beta$ RI)	ALK4 (ActRI-b), ALK7 (ActRI-c)	ALK1 (ACVRL1), ALK2 (Act-RI), ALK3 (BMPR-Ia), ALK6 (BMPR-Ib)
Type II receptors	TGF $\beta$ R2 (T $\beta$ RII)	ACVR2 (ActRII), ACVR2B (ActRIIb)	BMPR2 (BMPR-II), ACVR2 (ActRII), ACVR2B (ActRIIb)
Type III receptors	T $\beta$ RIII (betaglycan) CD105 (endoglin)	T $\beta$ RIII (betaglycan)	CD105 (endoglin)
R-SMADs	SMAD2/3	SMAD2/3	SMAD1/5/8
Co-SMAD	SMAD4	SMAD4	SMAD4
I-SMAD	SMAD7	SMAD7	SMAD6/7

<sup>a</sup> Based on [4].<sup>b</sup> Although type I receptors were initially called activin-receptor like kinases (ALKs), many have also been reported based on the subfamilies of signalling proteins where they belong to (given in brackets).

exert their function from an early stage of development and throughout adult life [5]. At a cellular level, the TGF $\beta$  family regulates embryonic development and cellular homeostasis, such as cell proliferation, differentiation, apoptosis, cytoskeletal organization, adhesion, and migration [6]. Members of the TGF $\beta$  family can also have various roles in later developmental events [4]. In mice with genetic alterations in TGF $\beta$  signalling, defects in haematopoiesis, as well as in cardiac, kidney, bone, liver, gastrointestinal tract, and gonadal development, were observed [4]. The TGF $\beta$  family of cytokines achieve homeostasis through a careful balance of complex signalling pathways that, following inappropriate activation, inhibition, or mutations in specific pathway components, could lead to diseases such as cancer, vascular diseases, and developmental disorders [4,6–13]. With such multifunctional roles, it provides not only many therapeutic targets, but also associated challenges, because inhibiting a pathological response can induce adverse effects elsewhere. Preclinical validated PET tracers that target the TGF $\beta$  pathway can provide insights into the expression levels of these targets in diseases. Thus, better understanding of the TGF $\beta$  pathway in specific diseases will provide insights into both the progression and state of the disease and as well as new opportunities for the development and evaluation of new therapies. In this review, we give an overview of PET tracers available to study the TGF $\beta$  signalling pathway. In addition, we also discuss future imaging targets for this pathway and possible leads for new PET tracers.

### Molecular PET imaging

PET imaging of molecules labelled with positron-emitting radionuclides (e.g. carbon-11, fluorine-18 and zirconium-89), has become a vital tool in current healthcare. PET allows for the study of disease biology, assists in drug development and disease detection in clinical practice, as well as treatment planning and monitoring. <sup>18</sup>F-fluoro-2-deoxyglucose (FDG) is one of the oldest and most widely used PET tracers in the clinic and was first described in 1975. The uptake of FDG is related to glucose metabolism and depends on the expression level of glucose transporters and hexokinase activity. In the clinic, FDG PET imaging is routinely used for cancer diagnosis, in particular for staging, but it can also be used in inflammation and other diseases where glucose metabolism is upregulated. In addition to FDG, other

PET tracers for oncological diagnosis have been developed and more are in development. Whereas FDG is a broadly applicable PET tracer, which provides information solely on glucose metabolism, novel tracers for oncology are more disease specific and only visualize, for example, a specific molecular target or pathway. Examples of this type of PET tracer are: [<sup>18</sup>F]DCFpyl for prostate-specific membrane antigen (PSMA) expression [14]; [<sup>11</sup>C]erlotinib for epidermal growth factor receptor (EGFR) expression [15]; [<sup>68</sup>Ga]FAPI tracers for the serine protease fibroblast activation protein [16]; and [<sup>89</sup>Zr]-DFO-trastuzumab for human EGF receptor (HER)2 expression [17]. PET imaging can also be used to study neurological, cardiological, and other diseases. For example, [<sup>18</sup>F]NaF is used for imaging bone diseases. Alzheimer's disease and plaques can be visualized using [<sup>11</sup>C]Pittsburg compound B (PIB), and [<sup>18</sup>F]N,N-diethyl-2-[4-(2-fluoroethoxy)phenyl]-5,7-dimethylpyrazolo[1,5-a]pyrimidine-3-acetamide (DPA714) has been developed to study translocator protein (TSPO) expression in neurological disorders [18,19]. PET imaging of specific targets has an advantage in that the molar activity (activity per unit mass) is so high that the activity that is needed for the imaging does not have a pharmacological effect. The mass dose for PET imaging is normally in the nmol range, which is orders of magnitude lower than that of computed tomography (CT) and magnetic resonance imaging (MRI). The mass doses of contrast agents used for these conventional imaging techniques are typically in the  $\mu$ mol to mmol range and, thus, can affect the system studied. In a preclinical setting, PET tracers are evaluated to assess whether they fulfil certain criteria. The positron-emitting radionuclide should not dissociate easily, otherwise imaging would follow the radionuclide rather than the tracer. In addition, the label should not alter the biological properties of the parent molecule, because this could result in a change in compound characteristics. Clearance of the tracer is also important, because it should be rapidly cleared from both nonspecific target sites and blood to allow for a signal that is dominated by specific binding, resulting in high tissue:background ratios. Within a clinical setting, tracers are evaluated in small proof-of-concept pilot studies for their safety and the presence of signal. When a tracer is deemed safe, it can be evaluated for its potential to image staging of a disease, in the prediction of treatment response, or in the selection of the appropriate drug in a larger study. A drawback of nuclear imaging is that it generally provides limited

anatomical information, which is elucidated by multimodality imaging, in which PET imaging is combined with CT or MRI.

### Pathway activation of the TGF $\beta$ family by their ligands

The mechanisms of TGF $\beta$  family signalling have been reviewed extensively by others and, therefore, are only discussed briefly here, focussing on the potential to image individual components of this pathway [20–25]. As a ligand, TGF $\beta$  binds to single transmembrane serine/threonine kinase receptors, which are divided into two receptor subfamilies, type I and type II. The structural domains of type II receptors adopt a similar fold as the type I receptors in the extracellular and intracellular domains (Fig. 1a) [30]. The function of the constitutively active type II receptors is to phosphorylate serine and threonine residues in the so-called 'glycine-serine rich (GS) domain' of the type I receptors, so that the ATP-binding pocket is suitable for ATP binding [6].

To activate the TGF $\beta$  family, a heteromeric complex of type I and type II transmembrane serine/threonine kinase receptors has to be assembled (Fig. 2) [26]. To obtain this heteromeric complex, the dimeric ligand first binds to the type II TGF $\beta$  receptor (T $\beta$ R<sub>II</sub>), which subsequently recruits the type I receptor to form an active tetrameric kinase receptor complex, comprising two pairs of each receptor type [5]. Each individual monomer of the dimeric ligand has contact sites for both type I and type II receptors (Fig. 1B) [27]. Endoglin lacks kinase activity, but it regulates binding and TGF $\beta$  signalling. It is a homodimeric membrane glycoprotein of 90–95 kDa comprising disulfide-linked dimers. Endoglin can bind to TGF $\beta$ 1, TGF $\beta$ 3, activin A, bone morphogenetic protein (BMP)-7, and BMP2, but to do so it requires co-expression of the respective ligand-binding kinase receptor partner [28]. TGF $\beta$  cannot bind endoglin on its own, but requires TGF $\beta$ R2 receptors, the activin

type II receptor (ACVR2) or ACVR2B. However, endoglin can bind to TGF $\beta$ R2 receptors in the absence of ligand and thereby modulate TGF $\beta$  signalling [28,29]. Betaglycan is structurally related to endoglin and an integral membrane protein with an estimated molecular weight of 100 kDa. It also lacks kinase activity, but contains large extracellular domains, hydrophobic transmembrane domains, and short cytoplasmic domains involving non-covalent interactions. Betaglycan can bind the ligands TGF $\beta$ 1, TGF $\beta$ 2, TGF $\beta$ 3, inhibin A, BMP2, BMP4, and BMP7 [31,32].

The phosphorylated (active) type I receptor directly phosphorylates two serine residues within the (S)XS motif at the C-terminal end of receptor-regulated downstream (R)-SMADs, also called, SMAD1, 2, 3, 5, and 8 (Fig. 2) [5].

SMADs are the downstream mediators responsible for signal transduction towards the nucleus and, thus, the biological response of TGF $\beta$ . Eight SMADs have been described and have two regions of homology at the N and C terminals, termed Mad-homology domains MH1 and MH2, respectively, which are connected with a proline-rich linker sequence. Even though all SMADs share similarities, they all have a distinct function within the cell. SMADs act in a pathway-restricted fashion and different members of the SMAD family have individual roles in downstream signalling. As such, the TGF $\beta$ /activin type I receptors (ALK4, -5, and -7), phosphorylate SMAD2 and 3, whereas the BMP receptors ALK1–3 and 6 phosphorylate SMAD1, 5, and 8 [27]. After phosphorylation, individual SMADs dissociate from the type I receptor complex and associate with SMAD4. In the nucleus, SMAD complexes bind to specific DNA-binding sites, regulate downstream gene transcription, and mediate biological responses [5]. Negative regulation of TGF $\beta$  pathway activation takes place by inhibitory SMADs (i.e., SMAD6 and SMAD7). They either bind to type I

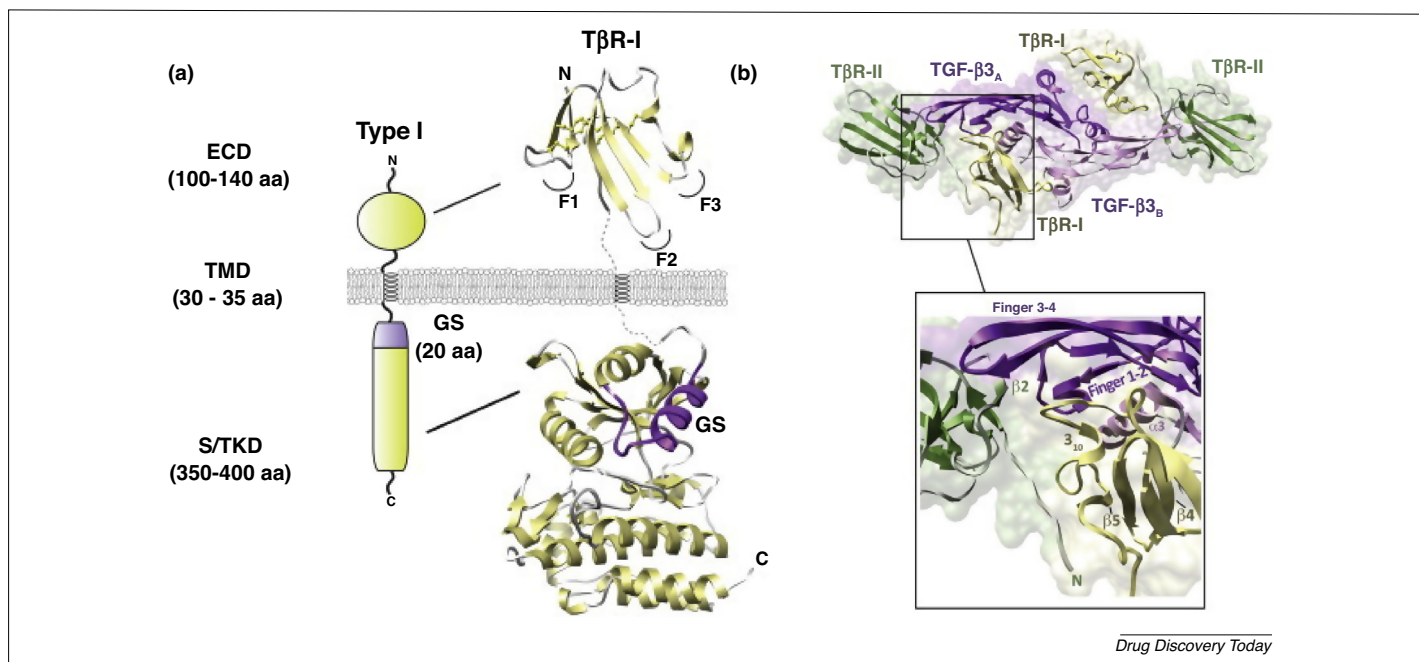


**FIGURE 1**

Structure of the transforming growth factor  $\beta$  receptor I (TGF $\beta$ RI). (a) The extracellular domain (ECD) of the ALK5 receptor, the transmembrane domain (TMD), the serine-threonine kinase domain (S/TKD), an ~20 amino acid juxtamembrane glycine-serine-rich regulatory domain (the GS box). (b) The TGF $\beta$  ternary complex structure of the transforming growth factor  $\beta$ 3 (TGF $\beta$ 3) in purple, the transforming growth factor  $\beta$  receptor I (T $\beta$ RI) in tan and the transforming growth factor  $\beta$  receptor II T $\beta$ RII in purple [30]. Reprinted, with permission, from [30].

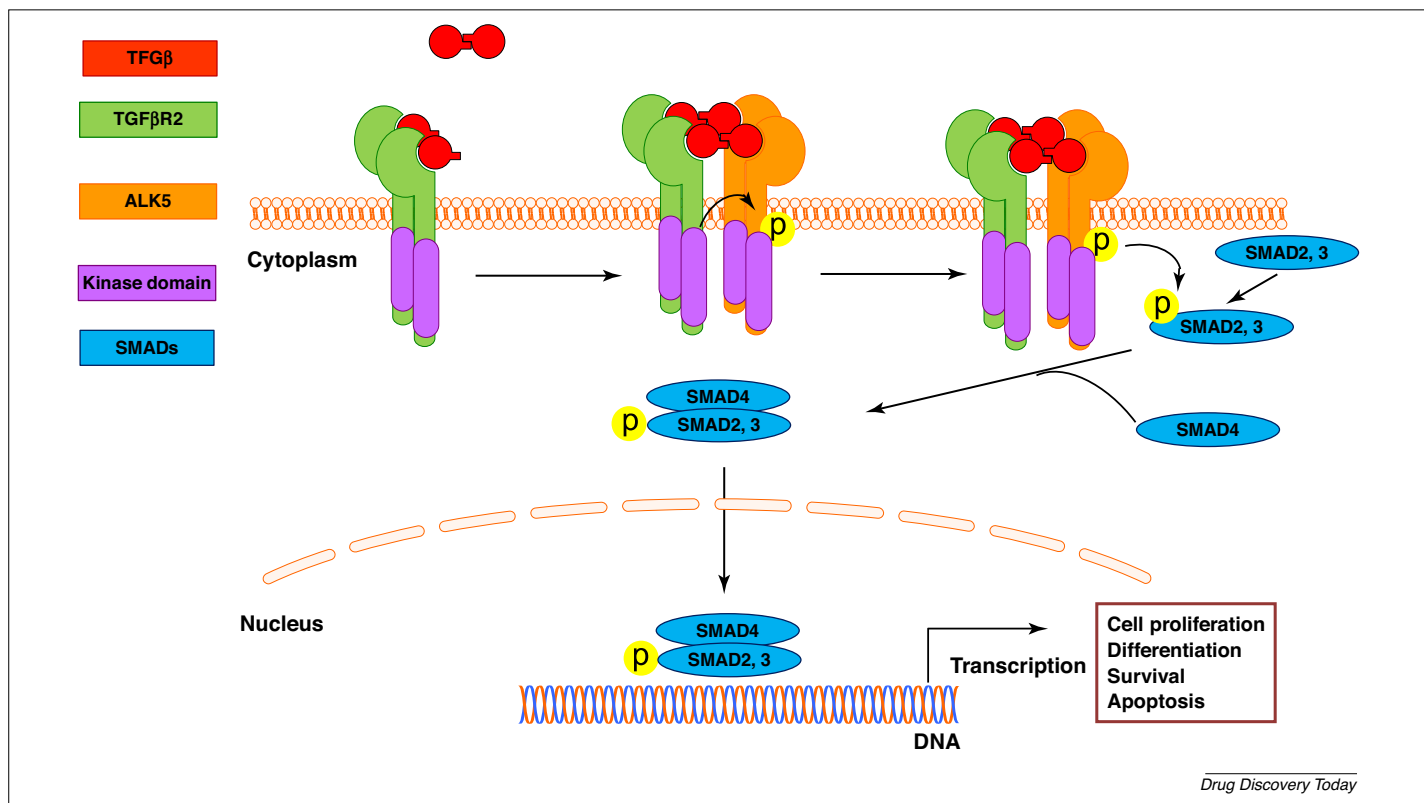


FIGURE 2

Signalling cascade of the transforming growth factor (TGF) $\beta$  pathway. Ligands are indicated in red, type I receptors in orange, type II receptors in green, and SMADs in blue.

receptors and hinder phosphorylation of the pathway-restricted SMADs or recruit E3 ubiquitin ligase SMURFs so that type I receptors are targeted for degradation by lysosomal and proteasomal degradation and no active heteromeric SMAD complexes can be generated [33]. TGF $\beta$  receptor-initiated SMAD-independent pathways can diverge into almost all other known classical signalling cascades, including small GTPases, the mitogen-activated protein kinase (MAPK) pathway and its various branches [extracellular signal-regulated kinase (ERK), Janus kinase (JNK), and p38], the phosphatidylinositol 3-kinase (PI3K) pathway, and various branches of the mitogen-activated protein kinase (MAPK) pathway [5]. Several mechanisms of crosstalk between pathways have been discovered. SMADs can be directly phosphorylated by MAPKs, SMADs can directly interact and modulate the activity of other signalling proteins, and TGF $\beta$  receptors can directly interact with or phosphorylate non-SMAD proteins, thus initiating parallel signalling that collaborates with the SMAD pathway in eliciting physiological responses [34]. Therefore, regulation of this pathway is not only under tight and complex control, both extracellularly and intracellularly, but also all components of the pathway (Fig. 3) and crosstalk with other pathways are involved in defining a role for how the TGF $\beta$  family signals and regulates cellular processes.

## The role of the TGF $\beta$ pathway in diseases

### Activating ligands of the TGF $\beta$ pathway

#### TGF $\beta$

TGF $\beta$  has a complex role in cancer biology, being involved in both tumour suppression and promotion. During the early stages of

tumour development, TGF $\beta$  is thought to be a tumour suppressor, but as the tumour evolves, cancer cells become resistant to its cytostatic effects and overexpression of TGF $\beta$  occurs within a tumour microenvironment that is conducive for tumour growth and metastasis development [35]. Furthermore, increased TGF $\beta$  activity occurs in patients with osteoarthritis, and fibrosis of the kidney, liver, heart, or lung [36–41]. In rats with restenosis after angioplasty, balloon catheterisation resulted in upregulated levels of TGF $\beta$  and TGF $\beta$  receptor types I and II. Active TGF $\beta$ 1 produced by smooth muscle cells was responsible for the early induction of integrins  $\alpha_v$  and  $\beta_3$  [42]. Clinically, however, decreased TGF $\beta$  activity was observed in patients with early tumour genesis, hereditary haemorrhagic telangiectasia (HTT), developmental defects, and atherosclerosis [43].

### Membrane regulators of the TGF $\beta$ pathway

#### Endoglin

Endoglin is a marker of actively proliferating tumour blood vessels and high endoglin expression is associated with poor prognosis in multiple tumour types [28]. Expression levels of endoglin can affect the response of endothelial cells to TGF $\beta$  and thereby modulate their proliferation. Endoglin can associate with TGF $\beta$ RII, thereby promoting cell proliferation and migration via the TGF $\beta$ /ALK1 signalling pathway and inducing inhibition of cell proliferation via the TGF $\beta$ /ALK5 signalling pathway [44–46].

#### Betaglycan

Betaglycan mediates and regulates cell migration, invasion, angiogenesis, apoptosis, and metastasis formation, all features that

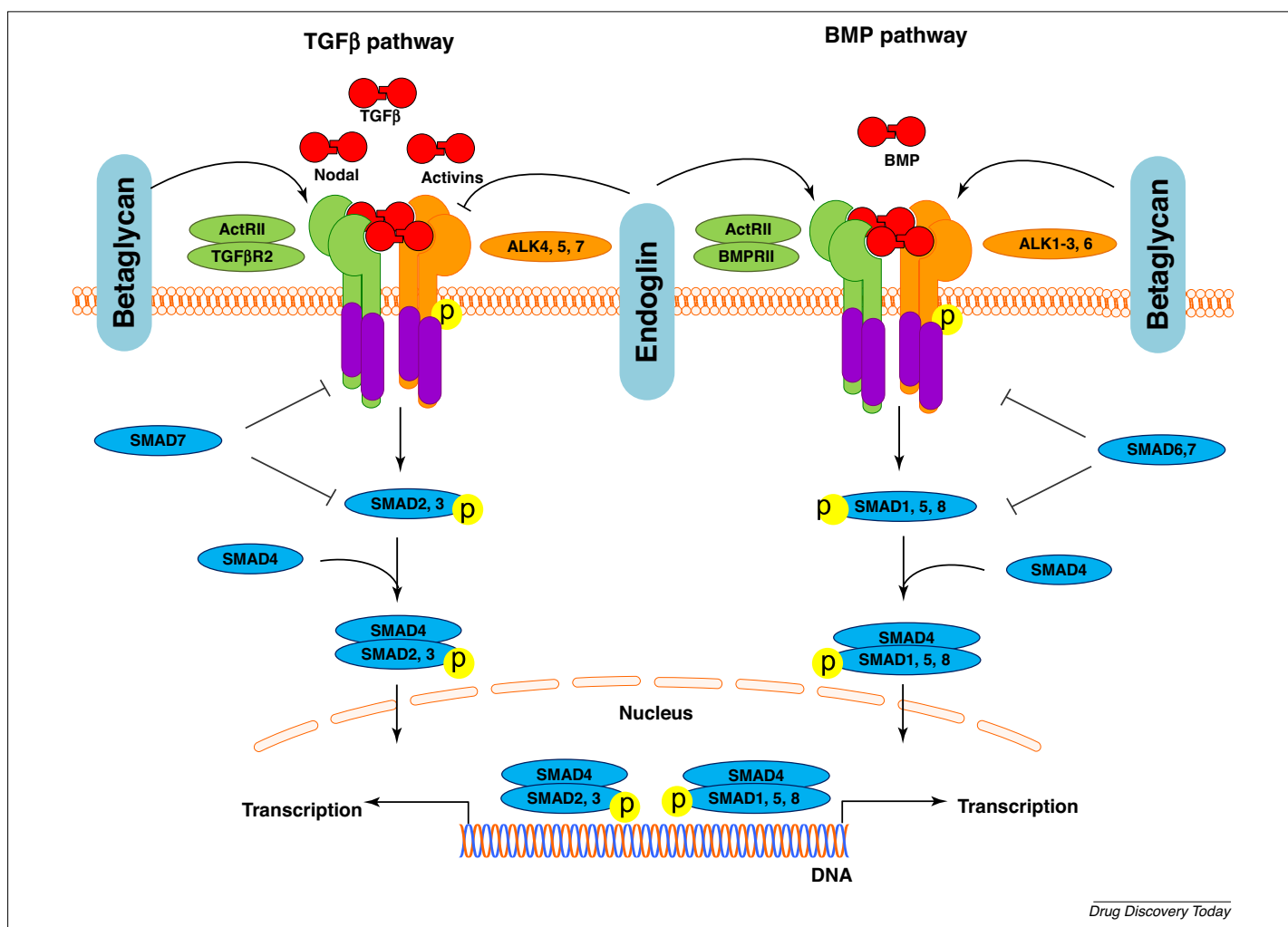


FIGURE 3

An overview of the transforming growth factor (TGF) $\beta$  family and their signalling mechanism based on their ligands and with respect to their relationship with each other. Ligands are indicated in red, type I receptor (TGF $\beta$ R1, also termed ALK5 (activin receptor-like kinase 5) in orange, type II receptor (TGF $\beta$ R2) in green, and SMADs in blue.

contribute to cancer progression. Decreased betaglycan expression suppresses cancer progression by reducing migration, invasion, and metastasis formation in *in vivo* tumour-bearing mouse models of breast, pancreatic, and non-small cell lung cancers [47–49]. In human pancreatic, ovarian, and renal cancer, decreased betaglycan expression has been observed in both mRNA and protein levels, and the degree of loss correlated with worsening tumour grade [48,50–52].

In colon cancer, increased betaglycan protein levels have been observed, whereas its mRNA expression levels were not altered, indicating post-transcriptional regulation of betaglycan expression [53].

#### TGF $\beta$ membrane receptors

##### TGF $\beta$ type I receptor (ALKs)

Elevated levels of the ALK5 receptor are found in numerous diseases, including pulmonary arterial hypertension, temporal lobe epilepsy, colonic fibrosis, osteosarcoma, pancreatic cancer, and breast cancer [54–59]. Pulmonary arterial smooth muscle cells (PASMCs) obtained from patients with familial pulmonary arterial hypertension (PAH) with defined BMPRII mutations were incubated with the potent ALK5 kinase inhibitor SB525334 to assess the contribution of ALK5 in mediating the abnormal TGF $\beta$  responses

observed in familial PAH PASMCs. The *in vitro* results indicated that PASMCs isolated from patients with PAH exhibited increased sensitivity to TGF $\beta$  compared with PASMCs from normotensive controls and that their elevated proliferation appeared to be mediated by ALK5 [58]. ALK5 expression has also been determined in tissue samples of the temporal neocortex from 30 patients with temporal lobe epilepsy. ALK5 protein expression in these samples was 2.4-fold higher than that in temporal lobe samples from nonepileptic controls. Immunohistochemistry showed that ALK5 was expressed mainly in astrocytes [55]. In two rat models of colonic fibrosis, increased protein levels of TGF $\beta$ 1, ALK5, and metalloproteinase inhibitor 1 were found in colon tissues. In addition, treatment of the animals with the ALK5 kinase inhibitor SD-208 downregulated SMAD2 and SMAD3 phosphorylation, and metalloproteinase inhibitor 1 and collagen deposition [56]. In human pancreatic cancer, all three TGF $\beta$  isoforms were found to be overexpressed [60]. In addition, mRNA levels of TGF $\beta$ R2 are also overexpressed in pancreatic cancers [61]. Balwin *et al.* reported that responsiveness to TGF $\beta$ 1 in cultured human pancreatic cancer cell lines correlated with the presence of high levels of ALK5 and that malignant cells within human pancreatic cancers

expressed high levels of TGF $\beta$ R2 and low levels of ALK5. In addition, treatment of breast cancer tumours in BALB/c *nu/nu* female mice with Ki26894, SD-208, and SD-093 demonstrated reduced tumour growth and decreased bone metastatic potential [54,62].

### TGF $\beta$ type II receptor (TGF $\beta$ R2)

Decreased levels of TGF $\beta$ R2 are associated with poor outcomes in patients with colon cancer, oesophageal cancer, or carcinoma of the lung [6]. Tissue microarrays of 310 colon carcinomas obtained from patients with curatively resected carcinomas in stages II and III were investigated for the expression of multiple TGF $\beta$  components. TGF $\beta$ 1 was found in 96% of the tumours. However, only a few tumours showed expression of TGF $\beta$ R1 (27%) and TGF $\beta$ R2 (5%). SMAD3 and SMAD4 were expressed in 91% and 100% of tumours, respectively. The main finding indicated that a decrease in both TGF $\beta$  receptors in tumour-associated stroma was associated with increased lymph node metastases and shorter survival [63]. To investigate the role of TGF $\beta$ R2 in pulmonary cancer, 48 premalignant bronchoepithelial lesions were obtained from patients at risk for, or with suspected, lung cancer. The progression of premalignant lesions towards carcinoma was accompanied by a decrease in TGF $\beta$ R2 expression [64]. In atherosclerotic lesions, decreased expression of the TGF $\beta$ R2 receptor was observed. Finally, cells derived from human vascular lesions have been compared with normal smooth muscle cells for their TGF $\beta$ R1, II, and III expressions. Cells were incubated with  $^{125}$ I-TGF $\beta$ 1 and a strikingly decrease in TGF $\beta$ R2 cell surface expression was observed. In addition, mRNA levels of TGF $\beta$ R2 were also decreased [65].

### Downstream targets within the TGF $\beta$ pathway

#### SMADs

High SMAD4 and low SMAD7 expression were found to be associated with better survival in patients with gastric cancer. Using tissue array methods in 304 consecutive patients with gastric carcinomas, positive SMAD4 expression was observed in 87.5% and positive SMAD7 expression in 32.2% of the tumours. The survival rate of patients with negative SMAD7 expression was significantly better than that of patients with positive SMAD7 expression [66]. Tissue microarray analysis was performed on 600 human colorectal cancer specimens to investigate SMAD2 and SMAD4 expression. Based on a comparison with the clinical outcome of the patients, it was concluded that a loss of SMAD2 and SMAD4 expression in colon cancer was associated with an advanced disease state, including lymph node metastasis and shorter survival rate [67]. In tumour tissue derived from patients with breast cancer, TGF $\beta$ 1, phosphorylated SMAD2/3, and SMAD4 were expressed in 50.9, 74.0, and 61.0% of samples, respectively. Loss of phosphorylated SMAD2/3 expression was associated with a shorter disease-free survival in all patients, and patients who did not express TGF $\beta$ 1 were 4.6 times more likely to experience distant recurrence [68]. Phosphorylated SMAD2 levels were determined in 52 patient-derived biopsies of astrocytomas of different grades obtained from surgical resection. In addition, TGF $\beta$ 1, TGF $\beta$ 2, TGF $\beta$ 3, Activin A, and Nodal levels were determined. A significant correlation was observed between phosphorylated SMAD2 levels and TGF $\beta$ 2. No correlations were observed between the other ligands. In addition, 25 gliomas of patients with a well-documented medical history were analysed and divided into two subgroups based on phosphorylated

SMAD2 levels. Higher levels of phosphorylated SMAD2 in gliomas were associated with poor prognosis [69].

### Molecular imaging

#### TGF $\beta$ pathway imaging

Given that the TGF $\beta$  pathway is widely involved in numerous diseases, its individual components have been targets for drug development for over a decade. Imaging the TGF $\beta$  pathway is an excellent means of gaining more insight into target expression, drug targeting, disease progression, and state of the disease as far as it is related to this pathway. This knowledge can, in turn, provide new opportunities for the development and evaluation of new therapies. To date, two components of the TGF $\beta$  pathway have been targeted for imaging: the TGF $\beta$  cytokine and the co-receptor endoglin, whereby imaging of the TGF $\beta$  cytokine was performed for drug development and endoglin was developed as potential diagnostic biomarker for cancer imaging. Here, we discuss different PET tracers and their application in several disease models. So far, the focus of imaging the TGF $\beta$  pathway has been on membrane receptors, which can be targeted with biologicals [e.g., monoclonal antibodies (mAbs) or fragments thereof]. To date, however, there have been no reports on attempts to image downstream or intracellular targets and no membrane-penetrating small molecules have been developed as PET tracers for the TGF $\beta$  pathway. This is interesting, given that many small-molecule kinase inhibitors that have been identified for TGF $\beta$ R kinases could easily serve as a basis for tracer development. Given the potential of these intracellular targets for imaging, their lead molecules are mentioned in the section 'Future imaging targets and possible leads for PET tracers'.

#### TGF $\beta$

Fresolimumab is a fully human IgG4  $\kappa$ -mAb capable of neutralizing TGF $\beta$ 1, TGF $\beta$ 2, and TGF $\beta$ 3. The safety of this biological was evaluated in patients with advanced malignant melanoma and renal cell carcinoma in a Phase I study [70]. In addition, a Phase II study was conducted in patients with mesothelioma [71]. After this study, Munnink *et al.* investigated the possibility of developing a PET tracer for imaging TGF $\beta$  [72]. Fresolimumab was labelled with zirconium-89 to obtain  $^{89}$ Zr-fresolimumab. Zirconium-89 was conjugated to fresolimumab through N-succinyl-desferrioxamine-B-tetrafluorophenol and used in a preclinical study, where tumour targeting of this PET tracer was examined in three different tracer concentrations (10, 50, and 100 mg) and in three different cancer types (Fig. 4). An *ex vivo* biodistribution study revealed similar uptake by the tumours of  $^{89}$ Zr-fresolimumab and  $^{111}$ In-IgG, where  $^{111}$ In-IgG reflected inflammation [72].

After successful preclinical imaging of TGF $\beta$  in Chinese hamster ovary (CHO) and breast cancer MDA-MB-231 xenograft-bearing mice, den Hollander *et al.* used  $^{89}$ Zr-fresolimumab PET in a clinical trial involving 12 patients with recurrent high-grade gliomas [73]. PET scans were acquired after 2 and 4 days post injection (p.i.) of the tracer. Afterwards, patients were treated with 5 mg/kg fresolimumab intravenously every 3 weeks. It was demonstrated that  $^{89}$ Zr-fresolimumab reached the tumours (Fig. 5). Unfortunately, patients had no benefit from treatment and treatment responses could not be correlated with tracer uptake [73].

#### Endoglin imaging

Endoglin is expressed on endothelial cells of both mature and immature blood vessels, with overexpression during angiogenesis,

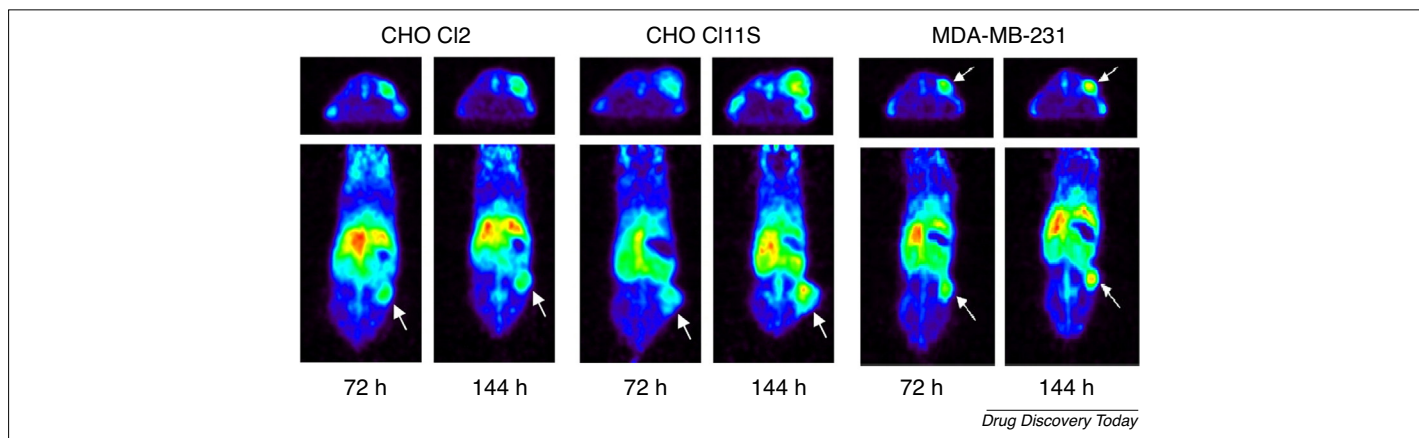


**FIGURE 4**

PET images of <sup>89</sup>Zr-fresolimumab in TGF-β-transfected Chinese hamster ovary (CHO CI2, high-expressing transforming growth factor (TGF)-β levels and CHO CI11S, lower expressing TGFβ levels) xenografts and MDA-MB-231 xenografts in mice [72]. Reprinted from [72].

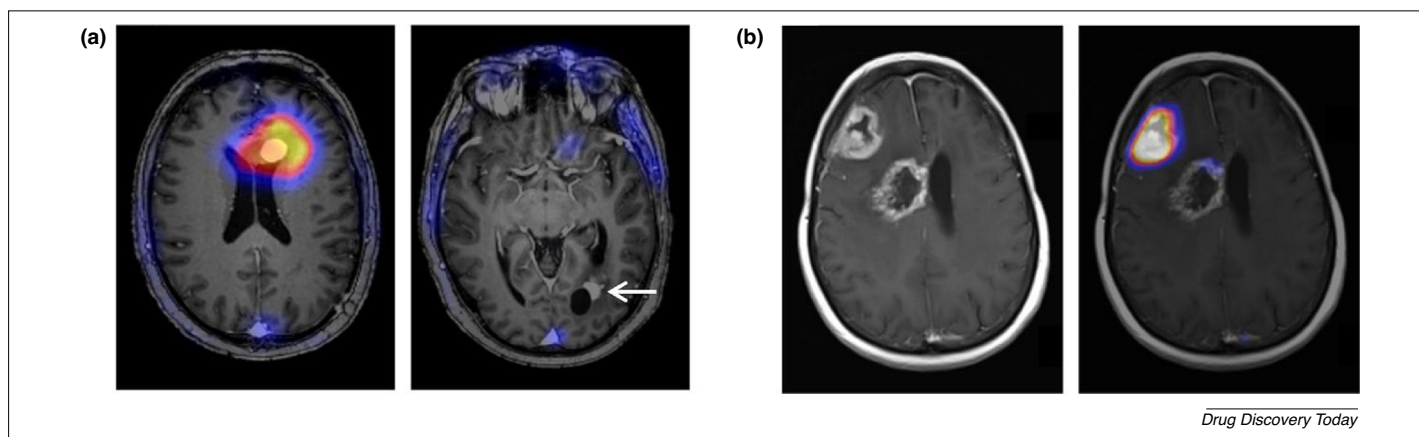


**FIGURE 5**

Positron emission tomography/magnetic resonance (PET/MR) images of patient with two contrast-enhancing lesions. (a) High uptake is visible in frontal lesion (i) but not in previously irradiated occipital lesion (ii). (B) SUV<sub>max</sub> was 5.5 in progressive right frontal lesion (i) and 2.1 in previously irradiated right paraventricular lesion (ii) [73]. Reprinted from [73].

**TABLE 2**

**Summary of reported PET antibodies targeting endoglin**

Antibody	Model	Refs
[ <sup>64</sup> Cu]Cu-NOTA-TRC105	4T1 murine breast cancer model	[77]
	Murine hindlimb Ischaemia model	[78]
	Rat myocardial infarction model	[79]
[ <sup>64</sup> Cu]Cu-DOTA-TRC105	4T1 murine breast cancer model	[79]
[ <sup>61</sup> Cu]Cu-NOTA-TRC105-Fab	4T1 murine breast cancer model	[85]
[ <sup>64</sup> Cu]Cu-NOTA-TRC105-Fab	4T1 murine breast cancer model	[85]
	Abdominal aortic aneurysm model	[86]
[ <sup>64</sup> Cu]Cu-NOTA – TRC105 – 800CW	4T1 murine breast cancer model	[87,88]
[ <sup>64</sup> Cu]Cu-NOTA-QD@HMSN-PEG-TRC105	4T1 murine breast cancer model	[89]
[ <sup>64</sup> Cu]Cu-NOTA-Bs-F(ab) <sub>2</sub>	U87MG tumour model	[90]
[ <sup>89</sup> Zr]Zr-Df-TRC105	4T1 murine breast cancer model	[91]
[ <sup>89</sup> Zr]Zr-Df-TRC105-800CW	4T1 murine breast cancer model	[92]
[ <sup>67</sup> Ga]Ga- endoglin	4T1 murine breast cancer model	[93]
[ <sup>86/90</sup> Y]Y-DTPA-TRC105	4T1 murine breast cancer model	[94]

leading to the assumption that **it** is a potential target for diagnostic imaging of solid tumours [74]. Multiple antibodies have been developed to target endoglin and some were labelled with the radiometals copper-61, copper-64, gallium-66, and zirconium-89 to develop a PET tracer (Table 2).

TRC105 is an endoglin-targeting antibody that showed anti-tumour activity in patients with advanced refractory solid tumours and prostate cancer [75,76]. Therefore, TRC105 and fragments of the antigen-binding (Fab) site of the antibody were labelled to image endoglin. This was accomplished by complexation of

copper-64, by using various different linkers and chelates. Tracer evaluation of [ $^{64}\text{Cu}$ ]Cu-DOTA-TRC105 Mab and [ $^{64}\text{Cu}$ ]Cu-NOTA-TRC105 Mab was performed in an 4T1 murine breast cancer model *in vivo*. The two conjugates showed similar targeting efficiency at 24 h p.i. However, when comparing *in vivo* data of both constructs, [ $^{64}\text{Cu}$ ]Cu-DOTA-TRC105 Mab uptake in liver, spleen and kidney was higher than that of [ $^{64}\text{Cu}$ ]Cu-NOTA-TRC105 Mab. Therefore, based on its lower background uptake, [ $^{64}\text{Cu}$ ]Cu-NOTA-TRC105 was superior for endoglin imaging [77]. [ $^{64}\text{Cu}$ ]Cu-NOTA-TRC105 has also been used to image angiogenesis in a murine hindlimb ischaemia model. Tracer uptake was significantly higher in the ischaemic hindlimb than in the nonischaemic contralateral hindlimb. In addition, tracer uptake in the ischaemic hindlimb increased significantly from the control level [ $1.6 \pm 0.2$  %ID/g to  $14.1 \pm 1.9$  %ID/g at Day 3 ( $N = 3$ )] and decreased with time to  $3.4 \pm 1.9$  %ID/g at Day 24, which correlated well with biodistribution studies at Days 3 and 24. Administration of a blocking dose of TRC105 2 h before [ $^{64}\text{Cu}$ ]Cu-NOTA-TRC105 injection significantly reduced tracer uptake in the ischaemic hindlimb at 48 h p.i., which confirmed the specificity of the tracer for endoglin *in vivo* (Fig. 6) [78].

[ $^{64}\text{Cu}$ ]Cu-NOTA-TRC105 has also been investigated for imaging myocardial infarction (MI) in a rat model. MI results in increased secretion of angiogenic factors to stimulate the formation of new blood vessels. Tracer uptake in the MI zone was significantly higher than in the control group ( $1.41 \pm 0.45$  versus  $0.57 \pm 0.07$  %ID/g;  $N = 3$ ,  $P < 0.05$ ) (Fig. 7). [ $^{64}\text{Cu}$ ]Cu-NOTA-TRC105 Mab displayed comparable uptake in the MI zone because the PET tracers targeted integrins (radiolabelled RGD peptide) and vascular endothelial growth factors [79–84].

To reduce the circulating lifetime of antibodies, the use of Fab or  $\text{F(ab')}_2$  fragments of TRC105 has also been studied. Labeled Fab or  $\text{F(ab')}_2$  fragments can yield higher imaging contrasts than intact antibodies at earlier time points. In studies with antibody fragments, copper-61 was also used as positron-emitting radionuclide because the short biological half-life of the fragments do not require the use of a long-lived isotope such as copper-64. Further-

more, copper-61 provides a stronger PET signal and a lower radiation dose compared with copper-64 because copper-61 has a higher  $\beta^+$  branching ratio (62 % versus 17 %) and a shorter physical half-life (3.4 h versus 12.7 h). Given that Fab fragments have rapid blood clearance and fast tumour uptake, a [ $^{61}\text{Cu}$ ]Cu-NOTA-TRC105-Fab was synthesized, evaluated *in vivo*, and compared with [ $^{64}\text{Cu}$ ]Cu-NOTA-TRC105-Fab. Tracers were injected in a 4T1 murine breast cancer model to quantify its tumour-targeting efficiency and normal organ distribution. Tumour uptake peaked earlier after tracer injection than for the intact antibody. [ $^{61}\text{Cu}$ ]Cu-NOTA-TRC105-Fab and [ $^{64}\text{Cu}$ ]Cu-NOTA-TRC105-Fab exhibited similar *in vivo* distribution patterns. [ $^{61/64}\text{Cu}$ ]Cu-NOTA-TRC105-Fab provided tumour contrast at 3 and 8 h after injection. Administration of a blocking dose significantly reduced tumour uptake of [ $^{64}\text{Cu}$ ]Cu-NOTA-TRC105-Fab (Fig. 8), illustrating its selectivity. These findings indicated that [ $^{64}\text{Cu}$ ]Cu-NOTA-TRC105-Fab binds selectively to CD105 *in vivo*. Given that tracer uptake of [ $^{61}\text{Cu}$ ]Cu-NOTA-TRC105-Fab is faster than that of [ $^{64}\text{Cu}$ ]Cu-NOTA-TRC105-Mab, this antibody-labelled fragment is suited for same-day immunoPET imaging [85].

[ $^{64}\text{Cu}$ ]Cu-NOTA-TRC105-Fab was also investigated in imaging abdominal aortic aneurysms in BALB/c mice. Uptake of the tracer was higher in the abdominal aortic aneurysm than in normal aorta. Furthermore, imaging showed that the extent of angiogenesis was stronger early during the disease [86]. In addition to tracers based on TRC105, dual-modality probes have been synthesised for combined nuclear and optical imaging. Optical imaging is a technique that uses light and photons to generate images of cellular and molecular functions in the body. The technique does not allow accurate quantification of the signal, but does provide better spatial resolution compared with PET. A combination of these two methods by synthesising a dual-modality agent can be used in the clinic, for example, in the context of image-guided surgery. [ $^{64}\text{Cu}$ ]Cu-NOTA-TRC105-800CW Mab was synthesised successfully and injected into a 4T1 murine breast cancer model with lung metastasis. The dual-modality agent could be used for both PET and optical imaging of endoglin expression in

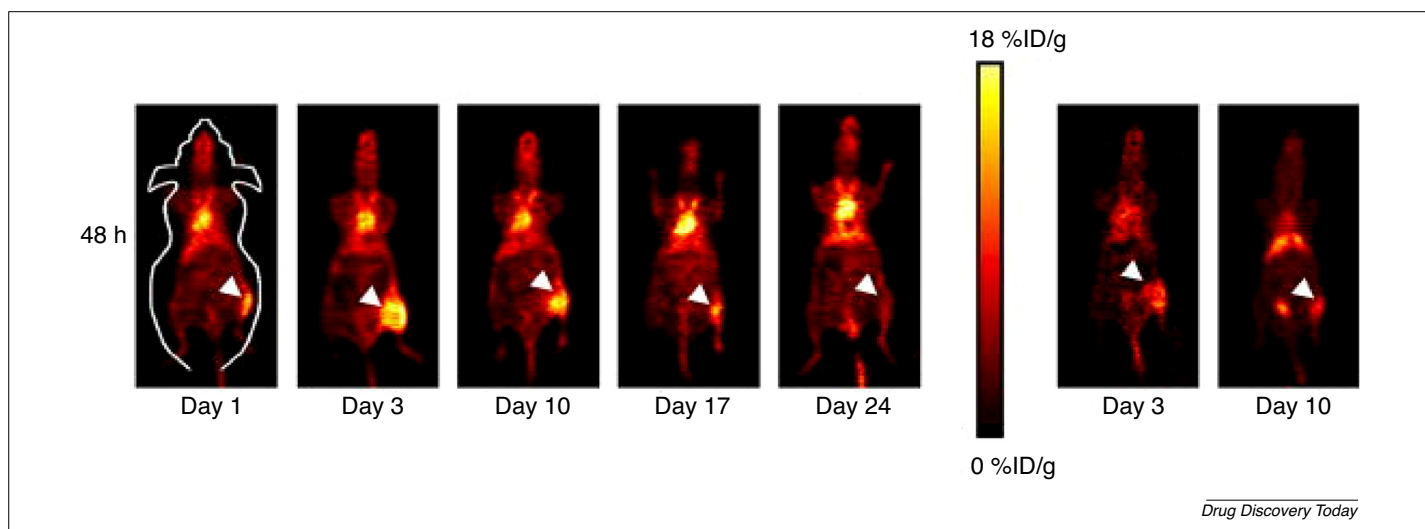


**FIGURE 6**

Positron emission tomography (PET) images at 48 h post injection of [ $^{64}\text{Cu}$ ]Cu-NOTA-TRC105 on days 1, 3, 10, 17, and 24 (a) after surgical creation of hindlimb ischaemia (arrowheads) and corresponding PET images of mice in the blocking group (b) on days 3 and 10 after surgery [78]. Reprinted from [78].

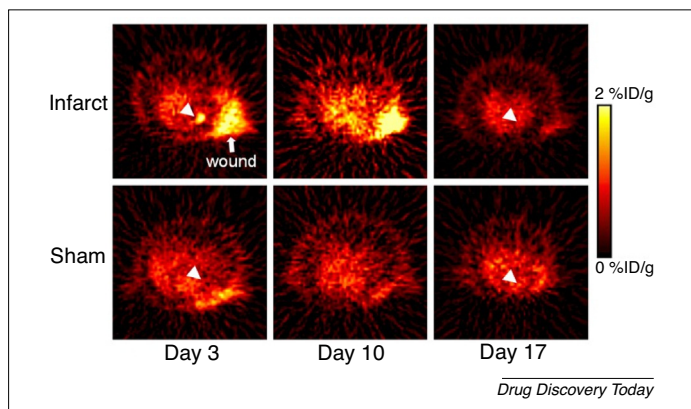


FIGURE 7

$^{64}\text{Cu}$  Cu-NOTA-TRC105 positron emission tomography (PET) images on days 3, 10 and 17 after surgery. Images were acquired at 48 h p.i. of the tracer. (a)

the breast cancer model, and small lung metastasis could be detected *in vivo* (Fig. 9) [87,88].

To enhance tumor targeting specificity a yolk/shell-structured silica nanosystem,  $^{64}\text{Cu}$  Cu-NOTA-QD@HMSN-PEG-TRC105, was developed for dual-modality PET/optical imaging of endoglin. Successful endoglin targeting was achieved that enhanced tumour retention and targeting specificity [89].

Luo et al. developed a dual-targeting immunoconjugate by linking two antibody Fab fragments against the epidermal growth factor receptor (EGFR) and an endoglin Fab fragment, via bioorthogonal 'click' ligation of *trans*-cyclooctene and tetrazine. This dual-targeting immunoconjugate was then labelled with copper-64 and injected into mice with U87MG tumours that express both EGFR and endoglin [90]. The uptake of the dual-labelled immunoconjugate was higher than that of the unattached Fab fragments [90].

An  $^{89}\text{Zr}$ -based PET tracer was developed for non-invasive imaging of endoglin expression by conjugating *p*-isothiocyanatobenzyl-desferrioxamine to TRC105 followed by labelling with zirconium-89. The tracer was injected into 4T1 breast tumour-bearing mice. Tumour uptake of  $^{89}\text{Zr}$  Zr-Df-TRC105 was visible

after 5 h p.i. and peaked around 24 h p.i.. A blocking dose of TRC105, administered 2 h before administering  $^{89}\text{Zr}$  Zr-Df-TRC105, reduced tumour uptake to background levels at all time points [91].

Zhang et al. developed a dual-modality PET and near-infrared fluorescence (NIRF) imaging agent for clinical diagnosis and for performing image-guided resections of solid tumours. TRC105 was conjugated to a NIRF dye (800CW) and to *p*-isothiocyanatobenzyl-desferrioxamine followed by  $^{89}\text{Zr}$ -labelling. The tracer was injected into 4T1 tumour-bearing mice and tumour uptake of  $^{89}\text{Zr}$  Zr-Df-TRC105-800CW was  $6.3 \pm 1.9$ ,  $12.3 \pm 1.3$ , and  $11.4 \pm 1.1$  %ID/g at 4, 24, and 48 h p.i., respectively ( $N = 3$ ). Administration of a blocking dose of TRC105 2 h before administration of  $^{89}\text{Zr}$  Zr-Df-TRC105-800CW reduced tumour uptake to background levels. Tumour uptake determined by NIRF imaging of the 4T1 tumour-bearing mice *in vivo* showed a linear correlation with the %ID/g values obtained by PET. As such, it appears that the NIRF scans provided relatively accurate quantification of tracer uptake in this model [92].

A  $^{66}\text{Ga}$ -based PET tracer has also been developed for imaging endoglin expression. TRC105 was conjugated to 2-*S*-(4-isothiocyanatobenzyl)-1-4-7-triazacyclononane-1,4,7-triacetic acid (*p*-SCN-Bn-NOTA) and labelled with gallium-66. PET imaging was performed using 4T1 tumour-bearing mice and tumour uptake of the tracer was  $5.9 \pm 1.6$ ,  $8.5 \pm 0.6$ , and  $9.0 \pm 0.6$  %ID/g at 4, 20 and 36 h p.i., respectively ( $N = 3$ ) [93]. Injection of a blocking dose of TRC105 reduced tumour uptake to  $4.4 \pm 1.2$ ,  $5.8 \pm 0.6$ , and  $7.2 \pm 0.6$  %ID/g at 4, 20 and 36 h p.i., respectively ( $N = 4$ ), which proved that a specific PET tracer had been developed [93].  $^{86/90}\text{Y}$  Y-DTPA-TRC105 was also developed for targeted imaging and therapy in neovasculature murine breast cancer models and to investigate the potential of  $^{86/90}\text{Y}$  Y-DTPA-TRC105 for theranostics, enabling precision treatment for cancer [94].

#### Downstream imaging of TGF $\beta$ activation

With respect to imaging the TGF $\beta$  pathway, the approach to visualise reporter genes is an indirect approach to image the desired target [95]. Repetitive monitoring of reporter gene

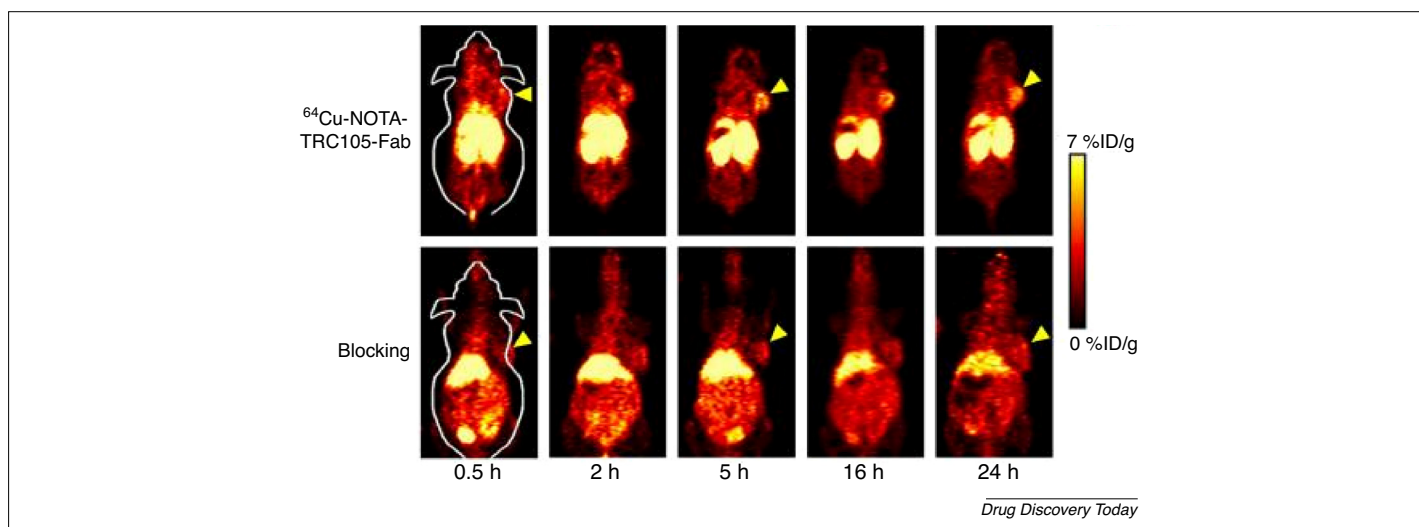
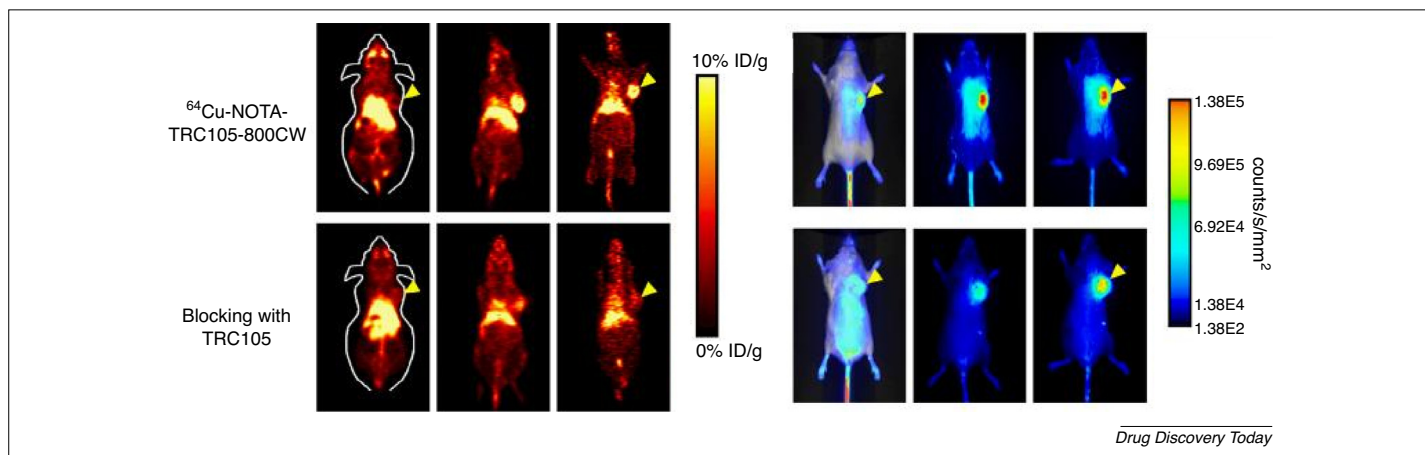


FIGURE 8

Positron emission tomography (PET) images at 0.5, 2, 5, 16 and 24 h p.i. of  $^{64}\text{Cu}$  Cu-NOTA-TRC105-Fab at baseline (i) and when co-injected with a 2 mg of TRC105-Fab [blocking (ii)] [85]. Reprinted, with permission from [85].

**FIGURE 9**

Positron emission tomography/near-infrared fluorescence (PET/NIRF) images of 4T1 tumour-bearing mice at 4, 24 and 48 h p.i. of [ $^{64}\text{Cu}$ ]Cu-NOTA-TRC105-800CW (i) and after blocking with 2 mg of TRC105 (ii). On the right serial NIRF images of the same mice as on the right [87]. Reprinted from [87].

expression can be applied for real-time monitoring of molecular events in intact living species [95]. For PET, both Herpes Simplex Virus Type-1 thymidine kinase (HSV1-tk) and dopamine type 2 can be transfected into the cells to be studied. It is also possible to apply multiple reporter genes with different imaging modalities (e.g., bioluminescence and PET) [95].

The general concept of this method is that cells should be cloned with a recombinant plasmid-containing imaging reporter gene under the control of a specific promoter. When transcription takes place, the reporter gene is introduced into the target. The amount of reporter protein is then an indirect measurement of the amount of target present in the cells and, when adding the imaging probe, the reporter protein can be visualised dynamically [96].

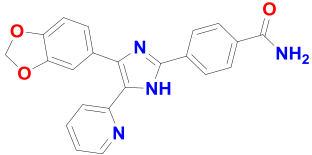
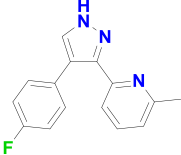
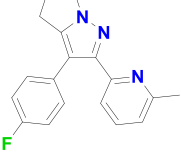
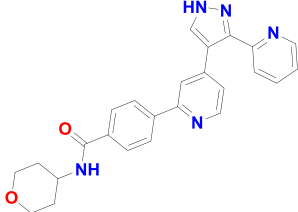
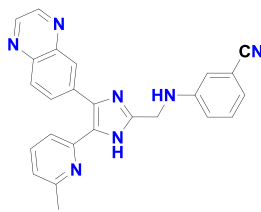
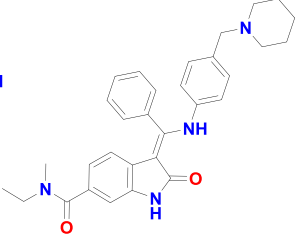
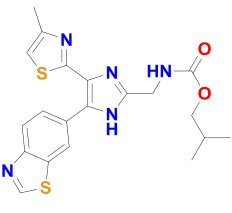
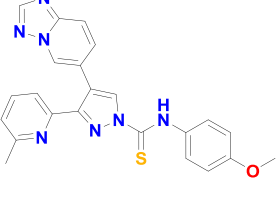
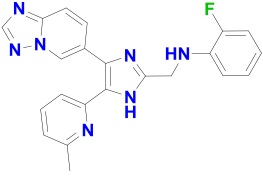
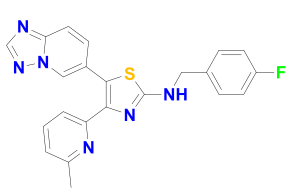
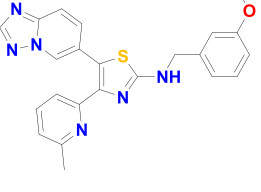
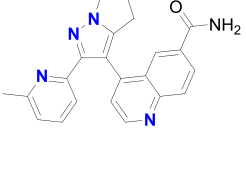
To obtain better insights into the localization and progression of metastases, and into the timing and course of TGF $\beta$  signalling, two MDA-MB-231 breast cancer cell lines with different metastatic tropisms, single cell-derived progeny 2 and 3 (SCP2 and SCP3), were cloned with constitutive and TGF $\beta$ -inducible reporter genes. The cells were injected intracardially *in vivo*, subsequently leading to metastasis formation in bone. The sites of metastasis expansion were visualized with bioluminescence imaging and TGF $\beta$  signalling was monitored using [ $^{18}\text{F}$ ]F-2'-Fluoro-5-Ethyl-Ara-U (FEAU). SCP2T cells developed rapidly growing metastases, primarily in bone, and SCP3T cells developed slowly growing metastases in the adrenal glands and bone. The advantage of this model is that a tomographic image data set can be obtained by co-registration of the corresponding  $\mu\text{CT}$  and PET images for combined volume-rendering imaging. In addition, exGluco bioluminescence imaging demonstrated higher sensitivity than  $\mu\text{PET}$  imaging and, thus, was suited for earlier detection of metastatic tumours. In conclusion, this technique can provide better insights into the initiation and kinetics of TGF $\beta$  activation, the localization of TGF $\beta$  signalling throughout the body, and the fluctuations in TGF $\beta$  signalling during growth of bone metastases [97].

### Potential imaging targets and possible leads for PET tracers

To date, multiple PET tracers of different components of the TGF $\beta$  family pathway have been developed to increase our understanding

of this signalling pathway in various diseases. However, the individual components that can be visualised currently represent only a small portion of the numerous components of the pathway. In addition, only extracellular components of the pathway have been targeted. Additional components could be imaged using either mAbs to visualise the extracellular domain of the receptors or small molecules to image intracellular downstream targets. The advantage of small molecules is that targeting occurs fast with rapid clearance from nontargeted organs. Tracers can be developed using radio-nuclides with shorter half-lives and results in a significantly reduced radiation dose for the study subjects. It also provides the opportunity to perform multiple imaging experiments within a relative short time and, in particular, pathway or molecular target quantification by dynamic scanning. The tracers must fulfil certain criteria besides good inhibitory potencies to make them potential PET tracers. Selectivity, stability, and ability to reach its target are also important for a PET tracer.

Initially, drug discovery focussed on the development of small molecules for the ALK5 receptor [13,98]. ALK5 inhibitors have been described with excellent inhibitory potencies ( $\text{IC}_{50}$  values  $<100$  nM), and high selectivities against the closely related p38 $\alpha$  MAPK. MAPK is one of the closest homologues to ALK5 in the ATP-binding pocket known outside the TGF $\beta$  pathway [99]. To date, developed ALK5 inhibitors all target the ATP-binding site of ALK5 and are catalogued as classical and nonclassical scaffolds. Classical scaffolds contain heterocycles, such as pyrazoles, imidazoles, and triazoles, whereas nonclassical scaffolds have other heterocycles, such as thiazoles [100–118]. Examples of scaffolds are depicted in Fig. 10, together with their  $\text{IC}_{50}$  values and selectivity indices (p38 $\alpha$   $\text{IC}_{50}$  and/or ALK5  $\text{IC}_{50}$ ). SB431542 developed by Callahan et al. [100] was one of the first highly selective ALK5 inhibitors that did not display p38 $\alpha$  MAPK inhibition. They performed a lead optimisation study using SB-203580 as starting point, an ALK5 inhibitor ( $\text{IC}_{50} = 0.40$  mM) and a p38 $\alpha$  MAPK inhibitor ( $\text{IC}_{50} = 0.49$  mM). The 4-pyridyl of SB-203580 was substituted for a 2-pyridyl group, thus preventing p38 $\alpha$  MAPK activation [100]. Compounds **1**, LY580276 and **2** were the lead structures of LY2157299 (galunisertib) which is currently under clinical investigation (Phase II) for the treatment of glioblastoma,

			
	SB431542	1	LY580276
IC <sub>50</sub> (nM)	94	70	175
Selectivity Index	> 178	> 286	>114
			
	2	IN-1166	3
IC <sub>50</sub> (nM)	18	12	34
Selectivity Index	> 404	85	8 % (p38α inhibition at 1 μM)
			
	4	5	EW-7197
IC <sub>50</sub> (nM)	5.5	0.6	7.0
Selectivity Index	-	11158	246
			
	6	7	Galunisertib
IC <sub>50</sub> (nM)	8.6	11	94
Selectivity Index	1069	>877	-

Drug Discovery Today

FIGURE 10

Examples of scaffolds for developing positron emission tomography (PET) tracers that target ALK5.

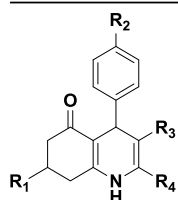
hepatocellular carcinoma, and myelodysplastic syndromes. In addition, clinical trials for glioma neoplasm metastasis and pancreatic neoplasms have been completed [119–126]. LY2157299 showed a positive pharmacokinetic and safety profile. In addition, tumour size decreased in patients with rectal cancer and glioblastomas [119–125]. IN-1166 (Fig. 10) was one of the first ALK5 inhibitors developed with a short linker between the core 5-membered heterocycle and the phenyl ring. This method has also been used in later designed scaffolds, such as compounds 4–7 and EW-7197 (Fig. 10) [106,114–117,127]. EW-7197 is under clinical investigation (Phase I) for the treatment of patients with advanced-stage solid tumours and displays favourable pharmacokinetics, with a  $K_i$  of

21 nM and a solubility profile in aqueous buffer at pH 1.2 (31.4 mg/ml) and 6.8 (0.042 mg/ml) [116]. Unfortunately, selectivity inside the TGFβ pathway of the inhibitors remains challenging because the ATP-binding sites of ALK4, ALK5, and ALK7 contain a large homology. Selectivity towards the TGFβ/ALK pathway is achieved based on the gatekeeper residue, ALK4, -5, and -7 all have the conserved gatekeeper residue S283, and ALK1, -2, -3, and -6 have T280 as a gatekeeper residue. By mutating the gatekeeper residue of ALK5 into T283, Ogunjimi et al. showed that SB431542 developed insensitivity towards the ALK5 receptor [128].

In addition, other drug development programs contributed to the development of small molecules that target the TGFβ

TABLE 3

## 1,4-Dihydropyridines inhibitors that target the TGFβRII [130,131]



Compound	R1	R2	R3	R4	IC <sub>50</sub> (nM)	Refs
8	<i>n</i> Pr	<i>t</i> Bu	COOEt	Me	170	[130]
9	(CH <sub>3</sub> ) <sub>2</sub>	<i>t</i> Bu	COOEt	NH <sub>2</sub>	510	[129]
10	(CH <sub>3</sub> ) <sub>2</sub>	Ph	CO <i>n</i> Pr	Me	500	[129]
11	(CH <sub>3</sub> ) <sub>2</sub>	4'-CH <sub>3</sub> Ph	COOEt	CH <sub>2</sub> NH <i>n</i> Pr	350	[129]

pathway. For TGFβRII, allosteric inhibitors have been developed with affinities in the nM range towards the TGFβRII receptor that do not target the ATP-binding site of the receptor. The advantage of these compounds (Table 3) is that they only target the TGFβRII receptor and have good selectivity over other receptors, even the closely related type I receptors. However, nonselective binding to other targets outside the TGFβ pathway has not yet been determined for these compounds, which makes them premature as potential inhibitors of this pathway and as PET tracers [129,130]. In addition, mAbs that target the TGFβ pathway are under development, such as IMC-TRI, which blocks the TGFβRII receptor; metelimumab and LY2382770, which target the TGFβ1 cytokine; and lerdelimumab, which targets the TGFβ2 cytokine [131–133].

### Concluding remarks and future perspectives

The complex TGFβ pathway regulates multiple cellular processes and an imbalance in this pathway results in numerous diseases, including fibrosis, cancer, pulmonary hypertension, HTT, and atherosclerosis. In a preclinical setting, non-invasive imaging of the different components of this pathway has been achieved, resulting in a better understanding of this pathway *in vivo*. This could lead to better precision medicine, because it is not always clear whether components of this pathway are up- or downregulated.

TGFβ and endoglin are the only targets of the TGFβ pathway that have been imaged so far, whereby only <sup>89</sup>Zr-fresolimumab has been applied in humans. Selective imaging of TGFβ was possible,

but patients did not benefit from treatment with fresolimumab and, thus, a predictive value for treatment responses could not be obtained. Significant effort has been put into imaging endoglin. Endoglin could selectively be imaged in cancer models, ischaemia models, MI, and aortic aneurysm by labelling different mAbs and fragment antibodies with copper-61, copper-64, zirconium-89 and gallium-66.

Direct imaging of the ALK5 receptor has yet to be accomplished. However, multiple small molecules have been described in drug discovery programs and, in principle, they are suited for radiolabelling with carbon-11 or fluorine-18 to obtain small-molecule PET tracers for visualisation of downstream targets of the TGFβ pathway. Another approach could be imaging of the TGFβRII receptor because most tumours retain TGFβRII expression. To accomplish this, more selective and potent inhibitors should be developed. In the future, direct imaging of the TGFβ receptors could provide better insights into the TGFβ pathway, which in turn could lead to precision medicine.

### Acknowledgements

We acknowledge the support from the Netherlands CardioVascular Research Initiative; the Dutch Heart Foundation, Dutch Federation of University Medical Centres, the Netherlands Organisation for Health Research and Development and the Royal Netherlands Academy of Sciences. P.t.D. is supported by Cancer Genomics Centre Netherlands (CGC.nl).

### References

- Willmann, J.K. *et al.* (2008) Molecular imaging in drug development. *Nat. Rev. Drug Discov.* 7, 591–607
- Rudin, M. and Weissleder, R. (2003) Molecular imaging in drug discovery and development. *Nat. Rev. Drug Discov.* 2, 123–131
- Massoud, T.F. and Gambhir, S.S. (2003) Molecular imaging in living subjects: seeing fundamental biological processes in a new light. *Genes Dev.* 17, 545–580
- Gordon, K.J. and Blobe, G.C. (2008) Role of transforming growth factor-beta superfamily signaling pathways in human disease. *Biochim. Biophys. Acta* 1782, 197–228
- Weiss, A. and Attisano, L. (2013) The TGFbeta superfamily signaling pathway. *Wiley Interdiscip. Re. Dev. Biol.* 2, 47–63
- Akhurst, R.J. and Hata, A. (2012) Targeting the TGF beta signalling pathway in disease. *Nat. Rev. Drug Discov.* 11, 790–811
- Border, W.A. and Noble, N.A. (1994) Transforming growth factor beta in tissue fibrosis. *N. Engl. J. Med.* 331, 1286–1292
- Feldmann, M. *et al.* (1996) Role of cytokines in rheumatoid arthritis. *Annu. Rev. Immunol.* 14, 397–440
- Böttinger, E.P. and Bitzer, M. (2002) TGF-beta signaling in renal disease. *J. Am. Soc. Nephrol.* 13, 2600–2610
- Aigner, L. and Bogdahn, U. (2008) TGF-beta in neural stem cells and in tumors of the central nervous system. *Cell Tissue Res.* 331, 225–241
- Rosenbloom, J. *et al.* (2013) Strategies for anti-fibrotic therapies. *Biochim. Biophys. Acta* 1832, 1088–1103
- Rabinovitch, M. (2008) Molecular pathogenesis of pulmonary arterial hypertension. *J. Clin. Invest* 118, 2372–2379
- Yingling, J.M. *et al.* (2004) Development of TGF-beta signalling inhibitors for cancer therapy. *Nat. Rev. Drug Discov.* 3, 1011–1022
- Chen, Y. *et al.* (2011) 2-(3-[1-Carboxy-5-(6- F-18 fluoro-pyridine-3-carbonyl)-amino-pentyl]-U reido)-pentanedioic acid, F-18 DCFPyL, a PSMA-based PET imaging agent for prostate cancer. *Clin. Cancer Res.* 17, 7645–7653

- 15 van Dongen, G.A. *et al.* (2012) PET imaging with radiolabeled antibodies and tyrosine kinase inhibitors: immuno-PET and TKI-PET. *Tumour Biol.* 33, 607–615
- 16 Loktev, A. *et al.* (2019) Development of novel FAP-targeted radiotracers with improved tumor retention. *J. Nucl. Med.* . <http://dx.doi.org/10.2967/jnumed.118.224469> Published online March 8, 2019
- 17 Holland, J.P. *et al.* (2010) Measuring the pharmacodynamic effects of a novel Hsp90 inhibitor on HER2/neu expression in mice Using Zr-DFO-trastuzumab. *PLoS One* 5, e8859
- 18 Nordberg, A. (2004) PET imaging of amyloid in Alzheimer's disease. *Lancet Neurol.* 3, 519–527
- 19 Sarda-Mantel, L. *et al.* (2012) Comparison of 18F-fluoro-deoxy-glucose, 18F-fluoro-methyl-choline, and 18F-DPA714 for positron-emission tomography imaging of leukocyte accumulation in the aortic wall of experimental abdominal aneurysms. *J. Vasc. Surg.* 56, 765–773
- 20 Miyazono, K. *et al.* (2005) BMP receptor signaling: transcriptional targets, regulation of signals, and signaling cross-talk. *Cytokine Growth Factor Rev.* 16, 251–263
- 21 de Caestecker, M. (2004) The transforming growth factor-beta superfamily of receptors. *Cytokine Growth Factor Rev.* 15, 1–11
- 22 Massagué, J. and Gomis, R.R. (2006) The logic of TGF beta signaling. *FEBS Lett.* 580, 2811–2820
- 23 Derynck, R. and Zhang, Y.E. (2003) Smad-dependent and Smad-independent pathways in TGF-beta family signalling. *Nature* 425, 577–584
- 24 Massagué, J. *et al.* (2005) Smad transcription factors. *Genes Dev.* 19, 2783–2810
- 25 Shi, Y. and Massagué, J. (2003) Mechanisms of TGF-beta signaling from cell membrane to the nucleus. *Cell* 113, 685–700
- 26 Villapol, S. *et al.* (2013) Role of TGF- $\beta$  signaling in neurogenic regions after brain injury. In *Trends in Cell Signaling Pathways in Neuronal Fate Decision* (Wislet, S., ed.), pp. 3–36, IntechOpen
- 27 Massagué, J. *et al.* (2000) TGF beta signaling in growth control, cancer, and heritable disorders. *Cell* 103, 295–309
- 28 Barbara, N.P. *et al.* (1999) Endoglin is an accessory protein that interacts with the signaling receptor complex of multiple members of the transforming growth factor-beta superfamily. *J. Biol. Chem.* 274, 584–594
- 29 Dallas, N.A. *et al.* (2008) Endoglin (CD105): a marker of tumor vasculature and potential target for therapy. *Clin. Cancer Res.* 14, 1931–1937
- 30 Hinck, A.P. (2012) Structural studies of the TGF-bs and their receptors - insights into evolution of the TGF-b superfamily. *FEBS Lett.* 586, 1860–1870
- 31 Bernabeu, C. *et al.* (2009) The emerging role of TGF-beta superfamily coreceptors in cancer. *Biochim. Biophys. Acta* 1792, 954–973
- 32 Gatza, C.E. *et al.* (2010) Roles for the type III TGF-beta receptor in human cancer. *Cell. Signal.* 22, 1163–1174
- 33 Heldin, C.H. *et al.* (1997) TGF-beta signalling from cell membrane to nucleus through SMAD proteins. *Nature* 390, 465–471
- 34 Moustakas, A. and Heldin, C.H. (2005) Non-Smad TGF-beta signals. *J. Cell Sci.* 118, 3573–3584
- 35 Amerizadeh, F. *et al.* (2019) Current status and future prospects of transforming growth factor-beta as a potential prognostic and therapeutic target in the treatment of breast cancer. *J. Cell Biochem.* 120, 6962–6971
- 36 Siegel, P.M. and Massagué, J. (2003) Cytostatic and apoptotic actions of TGF-beta in homeostasis and cancer. *Nat. Rev. Cancer* 3, 807–820
- 37 Wakefield, L.M. and Roberts, A.B. (2002) TGF-beta signaling: positive and negative effects on tumorigenesis. *Curr. Opin. Genet. Dev.* 12, 22–29
- 38 Dumont, N. and Arteaga, C.L. (2003) Targeting the TGF beta signaling network in human neoplasia. *Cancer Cell* 3, 531–536
- 39 Thomas, M. *et al.* (2019) Losartan attenuates progression of osteoarthritis in the synovial temporomandibular and knee joints of a chondrodysplasia mouse model through inhibition of TGF-beta 1 signaling pathway. *Osteoarthritis Cartilage* 27, 676–686
- 40 Rao, S. and Mishra, L. (2019) Targeting transforming growth factor beta signaling in liver cancer. *Hepatology* 69, 1375–1378
- 41 Wang, R. *et al.* (2019) Novel molecular therapeutic targets in cardiac fibrosis: a brief overview. *Can. J. Physiol. Pharmacol.* 97, 246–256
- 42 Ward, M.R. *et al.* (1997) Inhibition of protein tyrosine kinases attenuates increases in expression of transforming growth factor-beta isoforms and their receptors following arterial injury. *Arterioscler. Thromb. Vasc. Biol.* 17, 2461–2470
- 43 Blobel, G.C. *et al.* (2000) Role of transforming growth factor beta in human disease. *N. Engl. J. Med.* 342, 1350–1358
- 44 Fonsatti, E. *et al.* (2010) Targeting cancer vasculature via endoglin/CD105: a novel antibody-based diagnostic and therapeutic strategy in solid tumours. *Cardiovasc. Res.* 86, 12–19
- 45 Goumans, M.J. *et al.* (2002) Balancing the activation state of the endothelium via two distinct TGF-beta type I receptors. *EMBO J.* 21, 1743–1753
- 46 Goumans, M.J. *et al.* (2009) TGF-beta signaling in vascular biology and dysfunction. *Cell Res.* 19, 116–127
- 47 Dong, M. *et al.* (2007) The type III TGF-beta receptor suppresses breast cancer progression. *J. Clin. Invest.* 117, 206–217
- 48 Gordon, K.J. *et al.* (2008) Loss of type III transforming growth factor beta receptor expression increases motility and invasiveness associated with epithelial to mesenchymal transition during pancreatic cancer progression. *Carcinogenesis* 29, 252–262
- 49 Finger, E.C. *et al.* (2008) TbetaRIII suppresses non-small cell lung cancer invasiveness and tumorigenicity. *Carcinogenesis* 29, 528–535
- 50 Hempel, N. *et al.* (2007) Loss of betaglycan expression in ovarian cancer: role in motility and invasion. *Cancer Res.* 67, 5231–5238
- 51 Copland, J.A. *et al.* (2003) Genomic profiling identifies alterations in TGFbeta signaling through loss of TGFbeta receptor expression in human renal cell carcinogenesis and progression. *Oncogene* 22, 8053–8062
- 52 Margulis, V. *et al.* (2008) Type III transforming growth factor-beta (TGF-beta) receptor mediates apoptosis in renal cell carcinoma independent of the canonical TGF-beta signaling pathway. *Clin. Cancer Res.* 14, 5722–5730
- 53 Gatza, C.E. *et al.* (2011) Type III TGF-b receptor enhances colon cancer cell migration and anchorage-independent growth. *Neoplasia* 13, 758–770
- 54 Baldwin, R.L. *et al.* (1996) Attenuated ALK5 receptor expression in human pancreatic cancer: correlation with resistance to growth inhibition. *Int. J. Cancer* 67, 283–288
- 55 Lu, Y. *et al.* (2009) Increased expression of TGFbeta type I receptor in brain tissues of patients with temporal lobe epilepsy. *Clin. Sci. (Lond.)* 117, 17–22
- 56 Medina, C. *et al.* (2011) Transforming growth factor-beta type I receptor (ALK5) and Smad proteins mediate TIMP-1 and collagen synthesis in experimental intestinal fibrosis. *J. Pathol.* 224, 461–472
- 57 Ehata, S. *et al.* (2007) Ki26894, a novel transforming growth factor-beta type I receptor kinase inhibitor, inhibits in vitro invasion and in vivo bone metastasis of a human breast cancer cell line. *Cancer Sci.* 98, 127–133
- 58 Thomas, M. *et al.* (2009) Activin-like kinase 5 (ALK5) mediates abnormal proliferation of vascular smooth muscle cells from patients with familial pulmonary arterial hypertension and is involved in the progression of experimental pulmonary arterial hypertension induced by monocrotaline. *Am. J. Pathol.* 174, 380–389
- 59 Sung, J.Y. *et al.* (2019) Upregulation of transforming growth factor-beta type I receptor by interferon consensus sequence-binding protein in osteosarcoma cells. *Biochim. Biophys. Acta Mol. Cell Res.* 1866, 761–772
- 60 Friess, H. *et al.* (1993) Enhanced expression of the type-II transforming growth-factor-beta in human pancreatic-cancer cells without alteration of the type-III receptor expression. *Cancer Res.* 53, 2704–2707
- 61 Friess, H. *et al.* (1993) Enhanced expression of transforming growth-factor beta isoforms in pancreatic-cancer correlates with decreased survival. *Gastroenterology* 105, 1846–1856
- 62 Ge, R. *et al.* (2006) Inhibition of growth and metastasis of mouse mammary carcinoma by selective inhibitor of transforming growth factor-beta type I receptor kinase in vivo. *Clin. Cancer Res.* 12, 4315–4330
- 63 Bacman, D. *et al.* (2007) TGF-beta receptor 2 downregulation in tumour-associated stroma worsens prognosis and high-grade tumours show more tumour-associated macrophages and lower TGF-beta1 expression in colon carcinoma: a retrospective study. *BMC Cancer* 7, 156
- 64 Muñoz-Antonia, T. *et al.* (2007) Expression of TGF beta Type-II receptor in association with markers of proliferation and apoptosis in premalignant lung lesions. *Cancer* 110, 1527–1531
- 65 McCaffrey, T.A. *et al.* (1995) Decreased type II type I TGF-beta receptor ratio in cells derived from human atherosclerotic lesions - Conversion from an antiproliferative to profibrotic response to TGF-beta 1. *J. Clin. Invest.* 96, 2667–2675
- 66 Kim, Y.H. *et al.* (2004) Prognostic significance of the expression of Smad4 and Smad7 in human gastric carcinomas. *Ann. Oncol.* 15, 574–580
- 67 Xie, W. *et al.* (2003) Loss of Smad signaling in human colorectal cancer is associated with advanced disease and poor prognosis. *Cancer J.* 9, 302–312
- 68 Koumoundourou, D. *et al.* (2007) Prognostic significance of TGF beta-1 and pSmad2/3 in breast cancer patients with T1-2,N-0 tumours. *Anticancer Res.* 27, 2613–2620
- 69 Bruna, A. *et al.* (2007) High TGF beta-Smad activity confers poor prognosis in glioma patients and promotes cell proliferation depending on the methylation of the PDGF-B gene. *Cancer Cell* 11, 147–160
- 70 Morris, J.C. *et al.* (2014) Phase I study of GC1008 (fresolimumab): a human anti-transforming growth factor-beta (TGF beta) monoclonal antibody in patients with advanced malignant melanoma or renal cell carcinoma. *PLoS One* 9, 11
- 71 Stevenson, J. *et al.* (2012) Phase II trial of anti-transforming growth factor-beta (TGF beta) monoclonal antibody GC1008 in relapsed malignant pleural mesothelioma (MPM). *Oncoimmunology* 30, 1
- 72 Oude Munnink, T.H. *et al.* (2011) PET with the Zr-89-labeled transforming growth factor-beta antibody fresolimumab in tumor models. *J. Nucl. Med.* 52, 2001–2008

- 73 den Hollander, M.W. *et al.* (2015) TGF-beta antibody uptake in recurrent high-grade glioma imaged with Zr-89-fresolimumab PET. *J. Nucl. Med.* 56, 1310–1314
- 74 Wikström, P. *et al.* (2002) Endoglin (CD105) is expressed on immature blood vessels and is a marker for survival in prostate cancer. *Prostate* 51, 268–275
- 75 Rosen, L.S. *et al.* (2012) A phase I first-in-human study of TRC105 (anti-endoglin antibody) in patients with advanced cancer. *Clin. Cancer Res.* 18, 4820–4829
- 76 Karzai, F.H. *et al.* (2015) A phase I study of TRC105 anti-endoglin (CD105) antibody in metastatic castration-resistant prostate cancer. *BJU Int.* 116, 546–555
- 77 Zhang, Y. *et al.* (2011) Positron emission tomography imaging of CD105 expression with a Cu-64-labeled monoclonal antibody: NOTA is superior to DOTA. *PLoS One* 6, 7
- 78 Orbay, H. *et al.* (2013) Positron emission tomography imaging of angiogenesis in a murine hindlimb ischemia model with Cu-64-labeled TRC105. *Mol. Pharm.* 10, 2749–2756
- 79 Orbay, H. *et al.* (2013) Positron emission tomography imaging of CD105 expression in a rat myocardial infarction model with (64)Cu-NOTA-TRC105. *Am. J. Nucl. Med. Mol. Imaging* 4, 1–9
- 80 Menichetti, L. *et al.* (2013) MicroPET/CT imaging of  $\alpha v \beta 3$  integrin via a novel  $^{68}\text{Ga}$ -NOTA-RGD peptidomimetic conjugate in rat myocardial infarction. *Eur. J. Nucl. Med. Mol. Imaging* 40, 1265–1274
- 81 Rodriguez-Porcel, M. *et al.* (2008) Imaging of VEGF receptor in a rat myocardial infarction model using PET. *J. Nucl. Med.* 49, 667–673
- 82 Gao, H. *et al.* (2012) PET imaging of angiogenesis after myocardial infarction/reperfusion using a one-step labeled integrin-targeted tracer  $^{18}\text{F}$ -AIF-NOTA-PRGD2. *Eur. J. Nucl. Med. Mol. Imaging* 39, 683–692
- 83 Higuchi, T. *et al.* (2008) Assessment of  $\alpha v \beta 3$  integrin expression after myocardial infarction by positron emission tomography. *Cardiovasc. Res.* 78, 395–403
- 84 Laitinen, I. *et al.* (2013) Comparison of cyclic RGD peptides for  $\alpha v \beta 3$  integrin detection in a rat model of myocardial infarction. *EJNMMI Res.* 3, 38
- 85 Zhang, Y. *et al.* (2013) PET imaging of CD105/endoglin expression with a Cu-61/64-labeled Fab antibody fragment. *Eur. J. Nucl. Med. Mol. Imaging* 40, 759–767
- 86 Shi, S. *et al.* (2015) PET Imaging of abdominal aortic aneurysm with Cu-64-labeled anti-CD105 antibody Fab fragment. *J. Nucl. Med.* 56, 927–932
- 87 Zhang, Y. *et al.* (2012) Positron emission tomography and optical imaging of tumor CD105 expression with a dual-labeled monoclonal antibody. *Mol. Pharm.* 9, 645–653
- 88 Zhang, Y. *et al.* (2013) Imaging tumor angiogenesis in breast cancer experimental lung metastasis with positron emission tomography, near-infrared fluorescence, and bioluminescence. *Angiogenesis* 16, 663–674
- 89 Shi, S. *et al.* (2018) In vivo tumor-targeted dual-modality PET/optical imaging with a yolk/shell-structured silica nanosystem. *Nanomicro Lett.* 10, 11
- 90 Luo, H. *et al.* (2015) Noninvasive brain cancer imaging with a bispecific antibody fragment, generated via click chemistry. *Proc. Natl. Acad. Sci. U. S. A.* 112, 12806–12811
- 91 Hong, H. *et al.* (2012) Positron emission tomography imaging of CD105 expression with Zr-89-Df-TRC105. *Eur. J. Nucl. Med. Mol. Imaging* 39, 138–148
- 92 Zhang, Y. *et al.* (2012) ImmunoPET and near-infrared fluorescence imaging of CD105 expression using a monoclonal antibody dual-labeled with Zr-89 and IRDye 800CW. *Am. J. Transl. Res.* 4, 333–346
- 93 Engle, J.W. *et al.* (2012) Positron emission tomography imaging of tumor angiogenesis with a Ga-66-labeled monoclonal antibody. *Mol. Pharm.* 9, 1441–1448
- 94 Ehlerding, E.B. *et al.* (2018) Y-86/90-based theranostics targeting angiogenesis in a murine breast cancer model. *Mol. Pharm.* 15, 2606–2613
- 95 Youn, H. and Chung, J.K. (2013) Reporter gene imaging. *Am. J. Roentgenol.* 201, W206–W214
- 96 Ray, P. *et al.* (2001) Monitoring gene therapy with reporter gene imaging. *Semin. Nucl. Med.* 31, 312–320
- 97 Serganova, I. *et al.* (2009) Multimodality imaging of TGF beta signaling in breast cancer metastases. *FASEB J.* 23, 2662–2672
- 98 Jiang, M.N. *et al.* (2018) 2D-QSAR study, molecular docking, and molecular dynamics simulation studies of interaction mechanism between inhibitors and transforming growth factor-beta receptor I (ALK5). *J. Biomol. Struct. Dyn.* 36, 3705–3717
- 99 Evers, P.A. *et al.* (1998) Conversion of SB 203580-insensitive MBP kinase family members to drug-sensitive forms by a single amino-acid substitution. *Chem. Biol.* 5, 321–328
- 100 Callahan, J.F. *et al.* (2002) Identification of novel inhibitors of the transforming growth factor beta 1 (TGF-beta 1) type 1 receptor (ALK5). *J. Med. Chem.* 45, 999–1001
- 101 Sawyer, J.S. *et al.* (2003) Synthesis and activity of new aryl- and heteroaryl-substituted pyrazole inhibitors of the transforming growth factor-beta type I receptor kinase domain. *J. Med. Chem.* 46, 3953–3956
- 102 Sawyer, J.S. *et al.* (2004) Synthesis and activity of new aryl- and heteroaryl-substituted 5,6-dihydro-4H-pyrazole 1,2-b pyrazole inhibitors of the transforming growth factor-beta type I receptor kinase domain. *Bioorg. Med. Chem. Lett.* 14, 3581–3584
- 103 Li, H.Y. *et al.* (2008) Optimization of a dihydropyrrlopyrazole series of transforming growth factor-beta type I receptor kinase domain inhibitors: discovery of an orally bioavailable transforming growth factor-beta receptor type I inhibitor as antitumor agent. *J. Med. Chem.* 51, 2302–2306
- 104 Li, H.Y. *et al.* (2006) Dihydropyrrlopyrazole transforming growth factor-beta type I receptor kinase domain inhibitors: A novel benzimidazole series with selectivity versus transforming growth factor-beta type II receptor kinase and mixed lineage kinase-7. *J. Med. Chem.* 49, 2138–2142
- 105 Gellibert, F. *et al.* (2006) Discovery of 4-[(4-3-(pyridin-2-yl)-1H-pyrazol-4-yl)pyridin-2-yl]-N-(tetrahydro-2H-pyran-4-yl)benzamide (GW788388): a potent, selective, and orally active transforming growth factor-beta type I receptor inhibitor. *J. Med. Chem.* 49, 2210–2221
- 106 Kim, D.K. *et al.* (2007) Synthesis and biological evaluation of 4(5)-(6-alkylpyridin-2-yl)imidazoles as transforming growth factor-beta type 1 receptor kinase inhibitors. *J. Med. Chem.* 50, 3143–3147
- 107 Bonafoux, D. *et al.* (2009) 2-Aminoimidazoles inhibitors of TGF-beta receptor 1. *Bioorg. Med. Chem. Lett.* 19, 912–916
- 108 Gellibert, F. *et al.* (2009) Design of novel quinazoline derivatives and related analogues as potent and selective ALK5 inhibitors. *Bioorg. Med. Chem. Lett.* 19, 2277–2281
- 109 Roth, G.J. *et al.* (2010) Design, Synthesis, and Evaluation of Indolinones as Inhibitors of the Transforming Growth Factor beta Receptor I (TGF beta RI). *J. Med. Chem.* 53, 7287–7295
- 110 Guckian, K. *et al.* (2010) Pyrazolone based TGF beta R1 kinase inhibitors. *Bioorg. Med. Chem. Lett.* 20, 326–329
- 111 Kim, D.K. *et al.* (2010) Synthesis and biological evaluation of 4(5)-(6-methylpyridin-2-yl)imidazoles and -pyrazoles as transforming growth factor-beta type 1 receptor kinase inhibitors. *Bioorg. Med. Chem.* 18, 4459–4467
- 112 Jin, C.H. *et al.* (2011) Synthesis and biological evaluation of 1-substituted-3(5)-(6-methylpyridin-2-yl)-4-(quinolin-6-yl)pyrazoles as transforming growth factor-beta type 1 receptor kinase inhibitors. *Bioorg. Med. Chem.* 19, 2633–2640
- 113 Jin, C.H. *et al.* (2011) Synthesis and biological evaluation of 1-substituted-3(5)-(6-methylpyridin-2-yl)-4-(quinoxalin-6-yl)pyrazoles as transforming growth factor-beta type 1 receptor kinase inhibitors. *Eur. J. Med. Chem.* 46, 3917–3925
- 114 Amada, H. *et al.* (2012) 5-(1,3-Benzothiazol-6-yl)-4-(4-methyl-1,3-thiazol-2-yl)-1H-imidazole derivatives as potent and selective transforming growth factor-beta type I receptor inhibitors. *Bioorg. Med. Chem.* 20, 7128–7138
- 115 Jin, C.H. *et al.* (2011) Synthesis and biological evaluation of 1-substituted-3-(6-methylpyridin-2-yl)-4-(1,2,4-triazolo 1,5-a pyridin-6-yl)pyrazoles as transforming growth factor-beta type 1 receptor kinase inhibitors. *Bioorg. Med. Chem. Lett.* 21, 6049–6053
- 116 Jin, C.H. *et al.* (2014) Discovery of N-((4-(1,2,4-Triazolo 1,5-a pyridin-6-yl)-5-(6-methylpyridin-2-yl)-1H-imidazol-2-yl)methyl)-2-fluoroaniline (EW-7197): a highly potent, selective, and orally bioavailable inhibitor of TGF-beta type I receptor kinase as cancer immunotherapeutic/antifibrotic agent. *J. Med. Chem.* 57, 4213–4238
- 117 Krishnaiah, M. *et al.* (2015) Synthesis and biological evaluation of 5-(fluoro-substituted-6-methylpyridin-2-yl)-4-(1,2,4-triazolo 1,5-alpha pyridin-6-yl)imidazoles as inhibitors of transforming growth factor-beta type I receptor kinase. *Bioorg. Med. Chem. Lett.* 25, 5228–5231
- 118 Niemeier, J.K. *et al.* (2014) Application of kinetic modeling and competitive solvent hydrolysis in the development of a highly selective hydrolysis of a nitrile to an amide. *Org. Process Res. Dev.* 18, 410–416
- 119 Brandes, A.A. *et al.* (2016) A Phase II randomized study of galunisertib monotherapy or galunisertib plus lomustine compared with lomustine monotherapy in patients with recurrent glioblastoma. *Neuro Oncol.* 18, 1146–1156
- 120 Rodon, J. *et al.* (2015) First-in-human dose study of the novel transforming growth factor-beta receptor I kinase inhibitor LY2157299 monohydrate in patients with advanced cancer and glioma. *Clin. Cancer Res.* 21, 553–560
- 121 Rodón, J. *et al.* (2015) Pharmacokinetic, pharmacodynamic and biomarker evaluation of transforming growth factor-beta receptor I kinase inhibitor, galunisertib, in phase 1 study in patients with advanced cancer. *Invest. New Drugs* 33, 357–370
- 122 Sepulveda-Sanchez, J. *et al.* (2015) Brain perfusion and permeability in patients with advanced, refractory glioblastoma treated with lomustine and the transforming growth factor-beta receptor I kinase inhibitor LY2157299 monohydrate. *Oncol. Lett.* 9, 2442–2448
- 123 Fujiwara, Y. *et al.* (2015) Phase 1 study of galunisertib, a TGF-beta receptor I kinase inhibitor, in Japanese patients with advanced solid tumors. *Cancer Chemother. Pharmacol.* 76, 1143–1152

- 124 Ikeda, M. *et al.* (2017) Phase 1b study of galunisertib in combination with gemcitabine in Japanese patients with metastatic or locally advanced pancreatic cancer. *Cancer Chemother. Pharmacol.* 79, 1169–1177
- 125 Ursino, M. *et al.* (2017) Dose-finding methods for Phase I clinical trials using pharmacokinetics in small populations. *Biom. J.* 59, 804–825
- 126 Ikeda, M. *et al.* (2019) A phase 1b study of transforming growth factor-beta receptor I inhibitor galunisertib in combination with sorafenib in Japanese patients with unresectable hepatocellular carcinoma. *Invest. New Drugs* 37, 118–126
- 127 Binabaj, M.M. *et al.* (2019) EW-7197 prevents ulcerative colitis-associated fibrosis and inflammation. *J. Cell Physiol.* 234, 11654–11661
- 128 Ogunjimi, A.A. *et al.* (2012) Structural basis for specificity of TGFβ family receptor small molecule inhibitors. *Cell Signal.* 24, 476–483
- 129 Längle, D. *et al.* (2015) Design, synthesis and 3D-QSAR studies of novel 1,4-dihydropyridines as TGFβ/Smad inhibitors. *Eur. J. Med. Chem.* 95, 249–266
- 130 Schade, D. *et al.* (2012) Synthesis and SAR of b-annulated 1,4-dihydropyridines define cardiomyogenic compounds as novel inhibitors of TGFβ signaling. *J. Med. Chem.* 55, 9946–9957
- 131 Zhong, Z. *et al.* (2010) Anti-transforming growth factor beta receptor II antibody has therapeutic efficacy against primary tumor growth and metastasis through multieffects on cancer, stroma, and immune cells. *Clin. Cancer Res.* 16, 1191–1205
- 132 Denton, C.P. *et al.* (2007) Recombinant human anti-transforming growth factor beta1 antibody therapy in systemic sclerosis: a multicenter, randomized, placebo-controlled phase I/II trial of CAT-192. *Arthritis Rheum.* 56, 323–333
- 133 Mead, A.L. *et al.* (2003) Evaluation of anti-TGF-beta2 antibody as a new postoperative anti-scarring agent in glaucoma surgery. *Invest. Ophthalmol. Vis. Sci.* 44, 334–3401